

# The adsorption of ethylene on Au/Pd(1 1 1) alloy surfaces

F. Calaza, F. Gao, Z. Li, W.T. Tysoe \*

*Department of Chemistry and Laboratory for Surface Studies, University of Wisconsin-Milwaukee, 3210 N Cramer Street, Milwaukee WI 53211, USA*

Received 3 July 2006; accepted for publication 30 October 2006

Available online 20 November 2006

## Abstract

The adsorption of ethylene on gold–palladium alloys formed on a Pd(1 1 1) surface is investigated using a combination of temperature-programmed desorption (TPD) and reflection absorption infrared spectroscopy (RAIRS). Various alloy compositions are obtained by depositing four monolayers of gold on a clean Pd(1 1 1) surface and annealing to various temperatures. For gold coverages greater than  $\sim 0.7$ , ethylene adsorbs primarily on gold sites, desorbing with an activation energy of less than 55 kJ/mol. At gold coverages between  $\sim 0.5$  and  $\sim 0.7$ , ethylene is detected on palladium sites in a  $\pi$ -bonded configuration (with a  $\sigma$ – $\pi$  parameter of  $\sim 0.1$ ) desorbing with an activation energy of between  $\sim 57$  and 62 kJ/mol. Further reducing the gold coverage leads to an almost linear increase in the desorption activation energy of ethylene with increasing palladium content until it eventually reaches a value of  $\sim 76$  kJ/mol found for ethylene on clean Pd(1 1 1). A corresponding increase in the  $\sigma$ – $\pi$  parameter is also found as the gold coverage decreases reaching a value of  $\sim 0.8$ , assigned to di- $\sigma$ -bonded ethylene as found on clean Pd(1 1 1).

© 2006 Elsevier B.V. All rights reserved.

*Keywords:* Infrared absorption spectroscopy; Chemisorption; Palladium gold alloy; Ethylene

## 1. Introduction

The synthesis of vinyl acetate monomer (VAM) from ethylene, acetic acid and oxygen is catalyzed by both supported palladium and palladium–gold alloys, where alloying with gold leads to a substantial increase in selectivity from  $\sim 85\%$  for pure palladium to approximately 92% for the alloy [1]. The reaction on Pd(1 1 1) has been shown to proceed via a pathway first proposed by Samanos in which ethylene reacts with adsorbed acetate species to form an acetoxyethyl–palladium intermediate, which yields VAM via a  $\beta$ -hydride elimination reaction [see Ref. [2] and references therein]. It has been proposed that reaction proceeds on the alloy at a site consisting of two gold atoms located at diagonally opposite corners of the square unit cell located on a (1 0 0) surface [3]. In order to further understand the effects of alloy formation on this reaction, the following

work explores the chemistry of ethylene on gold–palladium (1 1 1) alloy surfaces. This surface was selected for initial study since it has been demonstrated that various alloy compositions can be conveniently obtained by adsorbing  $\sim 4$  monolayers of gold onto a Pd(1 1 1) surface and annealing to various temperatures to cause gold to diffuse into the palladium substrate. This strategy therefore allows the chemistry of reactants on a relatively large numbers of alloy surface compositions to be compared. In addition, since this alloy system exhibits no additional ordered LEED patterns, it has been suggested that the gold and palladium atoms are randomly distributed at the surface thereby allowing correlations to be made between various surface Au–Pd ensembles and their chemical properties. This strategy was used, for example, to identify the size of the palladium ensemble required for acetylene cyclotrimerization [4].

The ethylene hydrogenation activity of gold–palladium alloys has been investigated theoretically using density functional theory (DFT), where it was found that the formation of the alloy reduced the ethylene heat of adsorption

\* Corresponding author. Tel.: +1 414 229 5222; fax: +1 414 229 5036.  
E-mail address: [wtt@uwm.edu](mailto:wtt@uwm.edu) (W.T. Tysoe).

[5]. Ethylene bonds in a di- $\sigma$  configuration on clean Pd(111) at low-temperatures where low-energy electron diffraction (LEED) measurements and DFT calculations show that it adsorbs at a bridge site [6–9]. The ethylene heat of adsorption is reduced at higher coverages to form  $\pi$ -bonded species. It has also been shown that the presence of sub-surface hydrogen on the Pd(111) surface induces the formation of  $\pi$ -bonded ethylene and LEED measurements reveal that this occupies an atop site [10,11]. It is therefore anticipated that both electronic and ensemble effects will influence the state of ethylene adsorption on gold–palladium-alloy surfaces.

## 2. Experimental

The apparatus used to collect reflection absorption infrared spectra (RAIRS) and temperature-programmed desorption (TPD) data have been described in detail elsewhere [12]. Briefly the sample cell used for the infrared experiments is constructed from a 2 3/4 six-way cube, which was oriented to allow infrared radiation to impinge onto the sample at the optimum 80° infrared incidence angle. The cell is attached to the main chamber *via* a gate valve which, when closed, completely isolates the infrared cell from the ultrahigh vacuum chamber and, when open, allows sample transfer into it. Spectra are collected with Bruker Equinox spectrometer, typically for 2000 scans at a resolution of 8 cm<sup>-1</sup>. TPD data were collected in another chamber that was equipped with a Dichor quadrupole mass spectrometer interfaced to a computer that allowed up to five masses to be monitored in a single experiment. The sample could be cooled to 80 K in both chambers by thermal contact to a liquid-nitrogen-filled reservoir and resistively heated to ~1200 K.

The Pd(111) single crystal was cleaned using a standard protocol and its cleanliness monitored using Auger spectroscopy and temperature-programmed desorption collected following oxygen adsorption [10]. Gold was evaporated from a small alumina tube [13], which enabled controlled and reproducible evaporation rates to be achieved. In order to precisely control the temperature of the gold, and therefore its evaporation rate, a C-type thermocouple was placed into the gold pellet. The amount of gold deposited onto the surface was monitored using Auger spectroscopy from the peak-to-peak intensities of the Au NVV and Pd MNN Auger features and the monolayer coverage was gauged from breaks in the gold uptake signal. The gold–palladium alloy was formed according to a recipe developed by Lambert et al. [4] by initially adsorbing four monolayers of gold then annealing to various temperatures for a period of five minutes in ultrahigh vacuum to produce the desired Au/Pd atomic ratio on the surface. The sample was then allowed to cool to 80 K, following which ethylene was adsorbed onto the surface at 80 K. The resulting variation in Auger peak-to-peak intensity with annealing temperature was in excellent agreement with previous work [4] and gold coverages are quoted

based on this calibration. The ethylene (Matheson, Research Grade) was transferred to glass bottles which were attached to the gas-handling line for introduction into the vacuum chamber.

## 3. Results

TPD data were collected at a heating rate of 3.7 K/s as a function of ethylene exposure to various gold–palladium alloy surfaces. Only ethylene desorption (27 amu) was detected and no other desorbing species, particularly hydrogen, were found. Ethylene was dosed from a capillary source to minimize the rise in background pressure and the gold–palladium alloy composition, as noted above, was gauged from the Auger spectra using the calibration curve constructed by Lambert et al. [4]. Note that since the electron-based spectroscopies used to construct this calibration may also contain contributions from layers deeper within the seldge, which presumably contain less gold, it may underestimate the amount of gold in the outer layer. Nevertheless, trends in the variation in gold coverage will correctly track the true values. Data were collected for gold coverages of 0.95, 0.90, 0.73, 0.5, 0.33, 0.17, 0.09, 0.05, and 0.03 monolayers, so that representative data are presented for selected coverages.

TPD data for a gold coverage of 0.73 (27% palladium) are displayed in Fig. 1a. In all cases, the ethylene exposures (in Langmuirs, 1 L = 1 × 10<sup>-6</sup> Torr s) are indicated on the figure. The desorption traces display a feature centered at ~227 K for low exposures with a peak temperature that decreases slightly with increasing ethylene coverage indicating repulsive interactions between adsorbed ethylene species. Note that only very small amounts of ethylene desorb at temperatures above ~150 K at higher gold coverages. Fig. 1b shows the effect of decreasing the gold coverage to 0.33 where ethylene desorbs at ~272 K at low-coverages and shifts and broadens to lower temperatures as the ethylene coverage increases so that, at a saturation ethylene coverage, ethylene desorbs in a broad state centered at ~229 K. Further decreasing the gold coverage to 0.09 (Fig. 1c) results in an increase in the low-coverage ethylene desorption activation energy so that the desorption peak temperature shifts to ~295 K. The ethylene desorption profile at higher exposures is now rather broad with a desorption rate maximum at ~218 K.

The low-ethylene-coverage TPD data are compared for all alloy surfaces in Fig. 2, which displays the desorption profiles as a function of gold coverage, following exposure to 0.25 L of ethylene, where the gold coverages are displayed adjacent to the corresponding spectra. This clearly shows the decreasing trend in desorption temperature with increasing gold coverage. The corresponding desorption activation energies are calculated using the Redhead equation [14] assuming a pre-exponential factor of 1 × 10<sup>13</sup> s<sup>-1</sup>, and the results are displayed in Fig. 3. These data confirm the decrease in ethylene desorption activation energy with increasing gold coverage. Note that, since ethylene

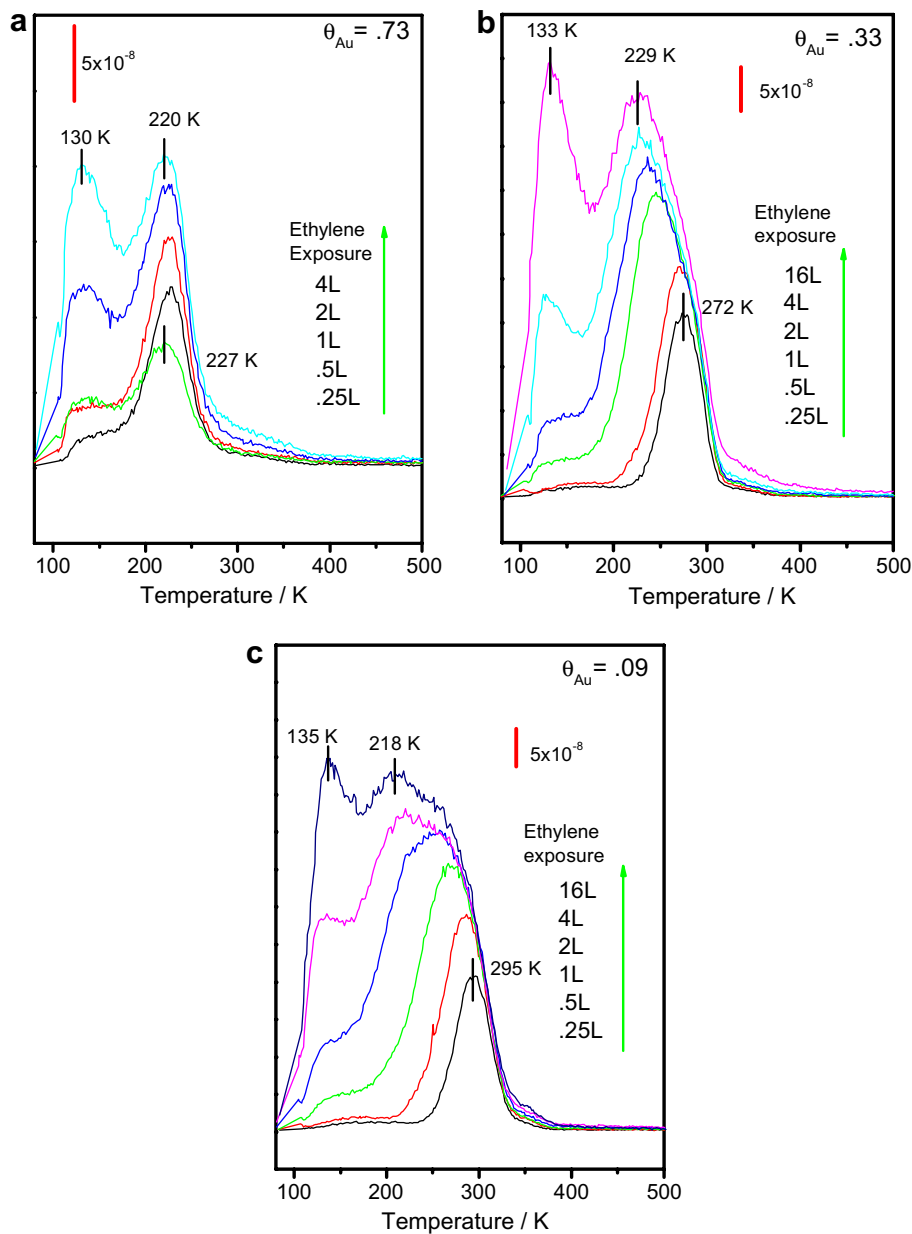


Fig. 1. Temperature-programmed desorption spectra for various exposures of ethylene adsorbed at 80 K on gold–palladium alloys with gold coverages of: (a) 0.73, (b) 0.33 and (c) 0.09, collected using a heating rate of 3.7 K/s. The ethylene exposures are marked adjacent to the corresponding spectrum.

adsorption is not strongly activated, these values will correspond closely to the heats of adsorption of ethylene on the various surfaces. Also indicated as arrows on this figure are the desorption activation energies for ethylene from clean Pd(111), where it adsorbs in a di- $\sigma$  configuration as well as on a hydrogen-covered surface, where it is  $\pi$ -bonded [15].

The corresponding TPD data for ethylene-saturated surfaces for various Au/Pd alloys are displayed in Fig. 4. This shows an initial increase in desorption temperature from  $\sim 218$  to  $\sim 230$  K as the gold coverage decreases from 0.73 to 0.5, close to the desorption temperatures measured at low exposures (Fig. 2). Ethylene desorbs from hydrogen-covered Pd(111) at  $\sim 230$  K, where this has been

shown to be due to  $\pi$ -bonded ethylene, implying that similar  $\pi$ -bonded species are also present on the surface at these gold coverages. However, the ethylene desorption feature at a gold coverage of 0.5 is broader than that at a gold coverage of 0.73 suggesting that the high-temperature tail in the former desorption profile may contain contributions from another, more strongly bound species. This trend is confirmed in the spectra for surfaces containing less gold, where a shoulder at  $\sim 300$  K is clearly discernible.

Selected RAIRS spectra for a saturated overlayer of ethylene adsorbed on various gold–palladium alloys at 80 K are displayed in Figs. 5 and 6 as a function of annealing temperature, where the annealing temperatures are dis-

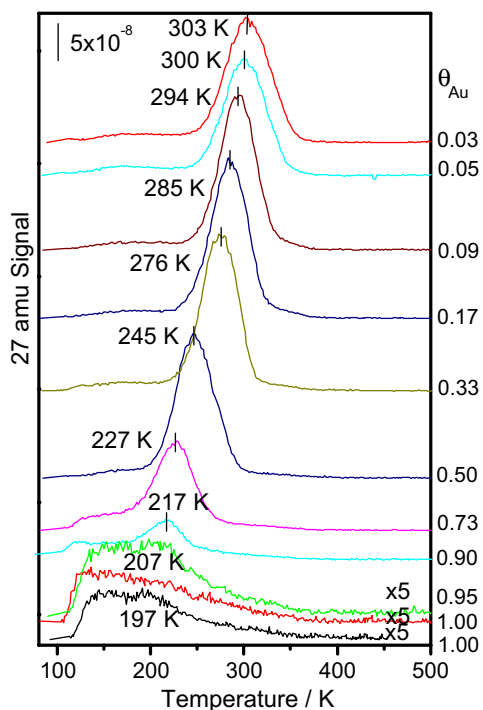


Fig. 2. Temperature-programmed desorption spectra for 0.25 L of ethylene adsorbed at 80 K on various gold–palladium alloys where the gold coverage is indicated adjacent to the corresponding desorption trace, collected using a heating rate of 3.7 K/s.

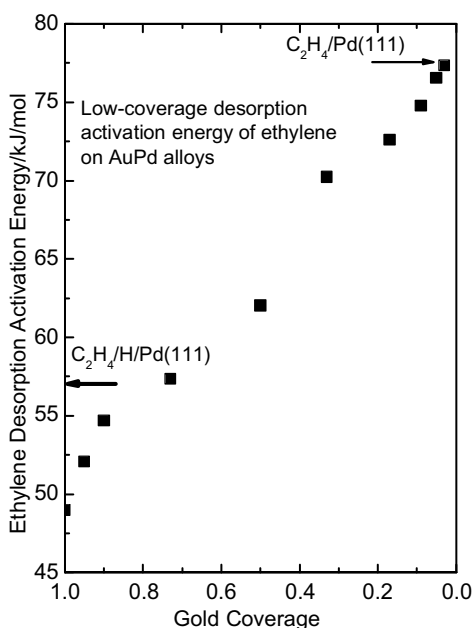


Fig. 3. Plot of the low-coverage desorption activation energy of ethylene on various gold–palladium alloys as a function of the gold coverage, where the desorption activation energies are calculated using the Redhead equation from the data of Fig. 4. Indicated for comparison are the corresponding desorption activation energies for di- $\sigma$  bonded ethylene from clean Pd(111) and for  $\pi$ -bonded ethylene from Pd(111)/H.

played adjacent to the corresponding spectrum. In these cases, the ethylene-covered samples were heated to the indi-

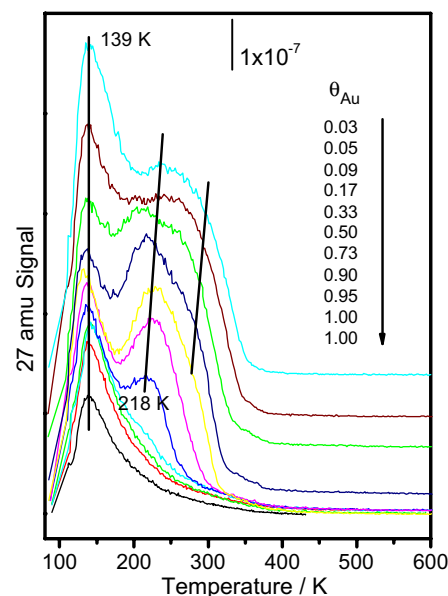


Fig. 4. Temperature-programmed desorption spectra for 16 L of ethylene adsorbed at 80 K on various gold–palladium alloys where the gold coverage is indicated adjacent to the corresponding desorption trace, collected using a heating rate of 3.7 K/s.

cated temperature for 5 s, then allowed to cool to 80 K, following which the spectrum was collected. A typical spectrum, in this case for a gold coverage of 0.95 is displayed in Fig. 5a. This displays a single feature at  $\sim 958\text{ cm}^{-1}$  assigned to the  $\text{CH}_2$  wagging mode of  $\pi$ -bonded ethylene [10]. The intensity of this feature decreases on heating so that it is completely absent after annealing to 172 K (data not shown) in good agreement with the desorption profile in Fig. 4. Fig. 5b displays the RAIR spectra for a surface with a gold coverage of 0.73, which shows a  $\sim 959\text{ cm}^{-1}$  feature following adsorption at 80 K. This decreases substantially in intensity on heating to 120 K, accompanied by the appearance of a feature at 931  $\text{cm}^{-1}$ , which is obscured by the intense  $959\text{ cm}^{-1}$  feature in the spectrum collected at 80 K. The  $959\text{ cm}^{-1}$  feature disappears completely on heating to  $\sim 216\text{ K}$ , indicating that it is associated with the low-temperature desorption feature in Fig. 4, while the  $931\text{ cm}^{-1}$  feature is still present at this temperature and is only removed by heating to 237 K (data not shown) indicating that this infrared feature is associated with the  $\sim 230\text{ K}$  desorption state (Figs. 2 and 4). This feature is again assigned to the  $\text{CH}_2$  wagging mode of  $\pi$ -bonded ethylene [10].

These features are still present on a surface with 50% gold (Fig. 5c) but now shifted slightly to 955 and  $926\text{ cm}^{-1}$ . Again the  $955\text{ cm}^{-1}$  feature disappears on heating to  $\sim 200\text{ K}$  confirming that it is associated with the low-temperature desorption state in the TPD data of Fig. 4, while the  $926\text{ cm}^{-1}$  peak is still present at 231 K, but disappears on heating to 262 K (data not shown) in accord with the TPD data of Figs. 2 and 4.

Further drastic changes occur as the gold coverage decreases further as shown in the data of Fig. 6. Now the

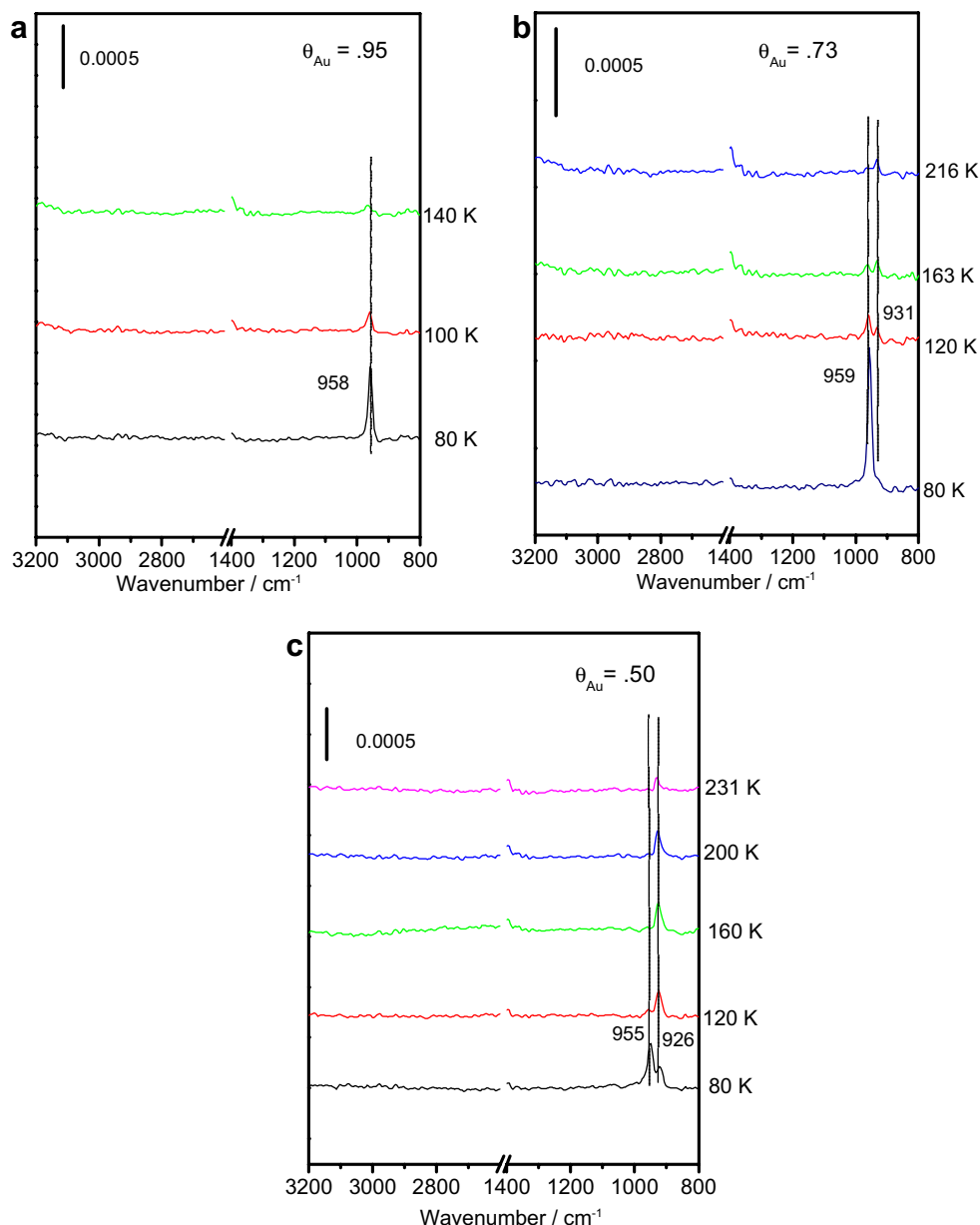


Fig. 5. Reflection-absorption infrared spectra of a saturated overlayer of ethylene on gold–palladium alloys with gold coverages of: (a) 0.95, (b) 0.73 and (c) 0.50 as a function of annealing temperature where the annealing temperatures are marked adjacent to the corresponding spectrum.

spectrum consists of an intense feature at  $\sim 903\text{ cm}^{-1}$  (Fig. 6a) with a weaker, but reproducible peak at  $1252\text{ cm}^{-1}$  for a gold coverage of 0.17. The  $903\text{ cm}^{-1}$  feature shifts to higher frequencies as the sample is heated so appears at  $\sim 926\text{ cm}^{-1}$  after annealing to 246 K, and disappears completely on heating to 278 K (data not shown), again in accord with the TPD data of Fig. 4. In addition, a weak but reproducible feature appears in the C–H stretching region at  $\sim 2962\text{ cm}^{-1}$ .

Additional changes for lower gold coverages are revealed in the data of Fig. 6b for a gold coverage of 0.09, where the most intense feature is at  $899\text{ cm}^{-1}$ , but shifts to higher frequencies when the sample is heated and displays an additional weak feature at  $\sim 1134\text{ cm}^{-1}$ .

These features persist until  $\sim 246\text{ K}$ , but are completely absent for a sample annealed to 278 K (data not shown), again in accord with the TPD results (Fig. 4). Again, a weak feature is detected in the C–H stretching region at  $\sim 2932\text{ cm}^{-1}$ .

Finally, the spectra for only a 5% gold coverage are displayed in Fig. 6c clearly showing the  $898$  and  $1111\text{ cm}^{-1}$  features as well as a clear  $2926\text{ cm}^{-1}$  mode in the C–H stretching region. Again the  $898\text{ cm}^{-1}$  mode shifts to higher frequencies as the sample is annealed to higher temperatures and the temperature at which the features disappear correspond well to the TPD spectrum (Fig. 4). The infrared feature at  $\sim 1100\text{ cm}^{-1}$  in this case is clearly indicative of the presence of di- $\sigma$  bonded ethylene [10].

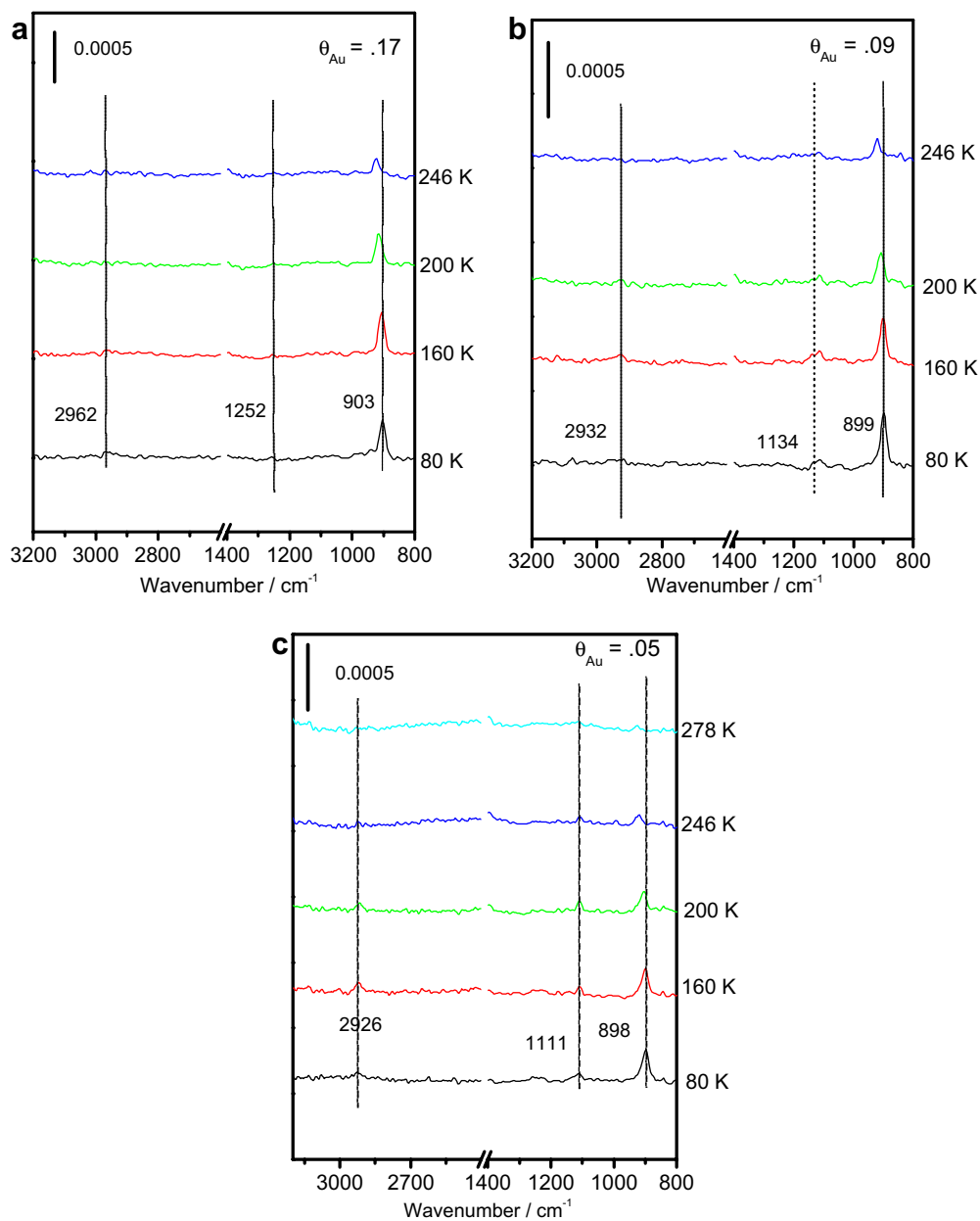


Fig. 6. Reflection-absorption infrared spectra of a saturated overlayer of ethylene on gold–palladium alloys with gold coverages of: (a) 0.17, (b) 0.09 and (c) 0.05 as a function of annealing temperature where the annealing temperatures are marked adjacent to the corresponding spectrum.

#### 4. Discussion

Ethylene adsorbs weakly on Au(111) surfaces exhibiting a  $\text{CH}_2$  wagging mode at  $\sim 960\text{ cm}^{-1}$  and desorbs below 200 K [3]. Extensive work has been carried out in ultrahigh vacuum on gold–palladium alloys either grown on low-index single crystal surfaces or as small alloy particles formed on model oxide thin films to mimic supported catalytic systems [16–19]. The majority of these studies have focused on alloys formed by the adsorption of palladium on gold single crystals surfaces where, for example, and ordered  $\sqrt{3} \times \sqrt{3}R30^\circ$  surface forms on Au(111) [20]. No ordered structures are found for the adsorption of gold onto palladium implying that the gold is rather randomly distributed

on the surface thus allowing random admixtures of different gold–palladium compositions to be obtained merely by annealing the sample to various temperatures. The ratio of Pd monomers to the total number of surface atoms for palladium on Au(111) has been measured experimentally using scanning tunneling microscopy [21] and yields good agreement with a random palladium distribution at low palladium coverages.

Assuming such a random distribution indicates that, for a gold coverage of 0.95, almost 90% of the palladium atoms are isolated yielding a total isolated palladium atom coverage, referenced to the total number of exposed atoms on the surface, of 4.5%. The weak ethylene desorption feature at  $\sim 207\text{ K}$  at this palladium coverage (Fig. 2) is therefore

assigned to desorption from palladium atoms completely surrounded by gold [22]. Experiments on the desorption of  $C_2D_4$  from Au–Pd/ $Al_2O_3$  model catalysts reveal that  $d_4$ -ethylene desorbs molecularly with a peak temperature increasing as the palladium content increases. In the case of an alloy containing predominantly gold,  $d_4$ -ethylene desorbs at  $\sim 215$  K, assigned to  $\pi$ -bonded ethylene adsorbed on isolated palladium sites [22]. In this case, because of the low palladium coverage, ethylene cannot be detected by RAIRS so that the infrared feature in Fig. 5a at  $\sim 958\text{ cm}^{-1}$  is therefore due to ethylene adsorbed on gold sites and this assignment is confirmed by the observation that this feature disappears on heating to  $\sim 172$  K. Ethylene has been found to desorb molecularly from clean and oxygen-covered Au(111), desorbing in a broad feature between 100 and 200 K [23] in agreement with this assignment.

The corresponding desorption peak shifts slightly and intensifies as the palladium coverage increases to  $\sim 0.1$  (Fig. 2). In this case, the proportion of isolated palladium atoms decreases to  $\sim 77\%$  giving a total coverage of isolated palladium atoms of  $\sim 7.7\%$  and the increase in ethylene desorption yield in Fig. 2 is in accord with this estimate. Again, such low ethylene coverages are not detectable by infrared spectroscopy.

Additional infrared features are detected at  $931\text{ cm}^{-1}$  appearing as a shoulder on the intense  $959\text{ cm}^{-1}$  feature assigned above to ethylene adsorbed on gold sites when the gold coverage decreases to 0.73 (Fig. 5b) and ethylene desorbs at  $\sim 227$  K from an alloy surface of this composition (Figs. 2 and 4). The  $931\text{ cm}^{-1}$  infrared feature is more clearly visible for a surface annealed to 120 K where the majority of the ethylene has desorbed from gold sites on the surface and is assigned to ethylene adsorbed on palladium sites. The  $931\text{ cm}^{-1}$  feature is approximately 10% as intense as the  $959\text{ cm}^{-1}$  peak. Since these are both due to  $CH_2$  wagging modes of  $\pi$ -bonded ethylene, the integrated areas of these features may be taken as a measure of the relative ethylene coverages on gold and palladium sites. If it is assumed that all exposed, isolated palladium atoms are occupied by  $\pi$ -bonded ethylene, then the ethylene coverage ratio on palladium sites ( $\Theta_{\text{ethylene}}(\text{Pd})$ ) to that on gold sites ( $\Theta_{\text{ethylene}}(\text{Au})$ ) is given by:

$$\frac{\Theta_{\text{ethylene}}(\text{Pd})}{\Theta_{\text{ethylene}}(\text{Au})} = \frac{\Theta(\text{Pd})}{\Theta(\text{Au})} \times P \quad (1)$$

where  $P$  is the proportion of the surface atoms that are isolated palladiums.  $\Theta(\text{Pd})/\Theta(\text{Au})$  is the ratio of the coverage of palladium to that of gold, and equals  $(1 - \Theta(\text{Au}))/\Theta(\text{Au})$  which, for the data of Fig. 5b is 0.37. The probability of a palladium atom being isolated is  $\sim 0.5$  [21] so that the ratio  $\Theta_{\text{ethylene}}(\text{Pd})/\Theta_{\text{ethylene}}(\text{Au})$  is  $\sim 19\%$ , larger than that found from the intensity ratios of the corresponding infrared features ( $\sim 10\%$ ) so that less  $\pi$ -bonded ethylene is formed on palladium sites than would be expected from a simple model that assumes that the gold and palladium atoms are randomly distributed. This model also assumes

that ethylene adsorbs on all atop sites on the gold surface while the saturation coverage of ethylene on gold is likely to be substantially less than unity leading to an even larger discrepancy between the measured and calculated coverages of  $\pi$ -bonded ethylene on gold and palladium sites.

A similar discrepancy is found for palladium coverages of 50% (Fig. 5c). In the case of random intermixing of gold and palladium, the number of each type of site should be identical leading to equal coverages of ethylene on both sites, while  $(\Theta_{\text{ethylene}}(\text{Pd})) / (\Theta_{\text{ethylene}}(\text{Au}))$  in this case is  $\sim 0.47$  rather than close to unity. These results imply that either the amount of gold on the surface is substantially underestimated, or the gold and palladium atoms are not randomly distributed, or that there are strong electronic effects that modify the reactivity of palladium sites.

A correlation diagram has been constructed for the vibrational frequencies of the symmetry-allowed modes of ethylene adsorbed on transition-metal surfaces as a function of the  $\sigma$ - $\pi$  parameter, where this parameter is defined to be equal to zero for purely  $\pi$ -bonded ethylene (with  $sp^2$  hybridized carbon) and unity for purely di- $\sigma$  bonded ethylene (with  $sp^3$  hybridized carbon) [24]. In this case, the C–C stretch,  $CH_2$  scissor and  $CH_2$  wagging modes of  $\pi$ -bonded ethylene correlate with the  $CH_2$  scissor,  $CH_2$  wagging and C–C stretching modes respectively of di- $\sigma$  bonded ethylene [10]. Of particular relevance in this case is the  $CH_2$  wagging mode (at  $949\text{ cm}^{-1}$  for gas-phase ethylene [10]), which moves to lower frequencies as the  $\sigma$ - $\pi$  parameter increases. This allows the degree of hybridization to be estimated for ethylene adsorbed on palladium. The results are displayed as a function of gold coverage in Fig. 7. The  $\sigma$ - $\pi$  parameter is  $\sim 0.12$  for gold coverages of 0.5 and 0.73, indicative of substantially  $\pi$ -bonded ethylene and these values are in good agreement with that of  $\pi$ -bonded ethylene on hydrogen-covered Pd(111) where LEED structure determinations have shown that the ethylene is, in this case, adsorbed on atop sites [6,10]. In addition, the desorption activation energies of ethylene from these alloy surfaces are close to that found for ethylene adsorbed on hydrogen-covered Pd(111) (see Fig. 3). Surface-enhanced Raman experiments carried out for ethylene adsorbed on gold-deposited noble metal films detected a  $CH_2$  wagging mode at  $\sim 934\text{ cm}^{-1}$  for  $\pi$ -bonded ethylene on gold corresponding to a calculated  $\sigma$ - $\pi$  parameter of  $\sim 0.28$  [25–27].

As the gold coverage decreases to  $\sim 0.17$ , the  $955\text{ cm}^{-1}$  infrared feature assigned to ethylene adsorbed on gold sites essentially disappears (Fig. 6a) since now the gold coverage is low. Furthermore, for gold coverages lower than  $\sim 0.4$ , the low-coverage ethylene desorption activation energy increases substantially (Figs. 2 and 3). This desorption feature is also evident as a shoulder on the desorption spectra collected at higher coverages (Fig. 4). The infrared spectrum for gold coverage of  $\sim 0.17$  exhibits an intense feature at  $903\text{ cm}^{-1}$ , along with much weaker features at  $\sim 1252$  and  $\sim 2962\text{ cm}^{-1}$  indicative of a  $\sigma$ - $\pi$  parameter of  $\sim 0.4$  (Fig. 7), and this change in carbon hybridization is in accord with the increase in ethylene adsorption energy

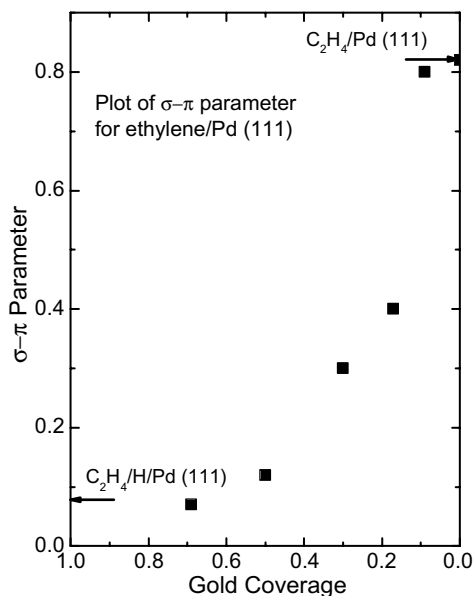


Fig. 7. Plot of the  $\sigma$ - $\pi$  parameter for ethylene on various gold-palladium alloys as a function of gold coverage, where the  $\sigma$ - $\pi$  parameters are calculated from the data in Ref. [10]. Indicated for comparison are the corresponding  $\sigma$ - $\pi$  parameters for di- $\sigma$  bonded ethylene on clean Pd(111) and for  $\pi$ -bonded ethylene on Pd(111)/H.

for a gold-palladium alloy surface of this compositions (Figs. 2–4). Di- $\sigma$  bonded ethylene on clean Pd(111) (with a  $\sigma$ - $\pi$  parameter of  $\sim 0.82$ ) displays an intense  $\text{CH}_2$  wagging mode at  $\sim 1100 \text{ cm}^{-1}$ , while the corresponding C–C stretching mode is much weaker. The mode at  $903 \text{ cm}^{-1}$  (Fig. 6a) appears therefore to be due to some  $\pi$ -bonded ethylene still present on the surface. As the gold coverage decreases even further to 0.09 (Fig. 6b) or 0.05 (Fig. 6c), this feature shifts to  $\sim 899 \text{ cm}^{-1}$ , but still remains as the most intense feature. The weak  $\text{CH}_2$  wagging mode shifts to  $\sim 1134 \text{ cm}^{-1}$  when the gold coverage is 0.09 and to  $1111 \text{ cm}^{-1}$  at  $\theta(\text{Au}) = 0.05$ , indicative of greater di- $\sigma$  bonding character as shown in Fig. 7 where the  $\sigma$ - $\pi$  parameter approaches that of clean palladium. This notion is borne of by the low-coverage activation energy (Figs. 2 and 3) where the ethylene heat of adsorption approaches that of clean palladium on surfaces with 9% or 5% gold. However, the infrared spectrum of ethylene on clean Pd(111) consists of a single feature at  $\sim 1100 \text{ cm}^{-1}$ , with no intensity at  $\sim 900 \text{ cm}^{-1}$  [10] while, with only a few percent of a monolayer of gold on the surface, the infrared spectrum still displays an intense feature at  $\sim 900 \text{ cm}^{-1}$  (Fig. 6c). Only by extensive argon ion bombardment at a sample temperature of 940 K to remove all remaining gold can the infrared spectrum of clean Pd(111) (displaying only a feature at  $\sim 1100 \text{ cm}^{-1}$ ) be recovered. This implies that only a very small amount of gold in the surface region has a profound effect on the adsorption properties of ethylene on the surface. As noted above, electron-based spectroscopies may not provide a completely accurate measure of the coverage of the outermost layer. However, it is clear from the low gold Auger and XPS signals for the sur-

faces used to collect the data shown in Fig. 6c, that the presence of  $\pi$ -bonded ethylene is induced by only a small amount of gold in the surface region clearly indicating that a small amount of gold alloyed with palladium drastically affects the electronic structure of palladium and correspondingly the heat of adsorption of ethylene. Low-energy ion scattering experiments are planned to more precisely determine the surface gold coverage. Nevertheless, it does appear that the adsorption of ethylene is affected by only a small amount of gold in the alloy. Since vinyl acetate is formed by insertion of ethylene into the O–Pd bond of acetate species, weaker bonding of ethylene to the surface is likely to facilitate this reaction.

## 5. Conclusions

Both TPD and RAIRS results indicate that alloying palladium with gold to form AuPd(111) surfaces has a profound effect on the adsorption of ethylene. For gold coverages greater than  $\sim 0.7$ , only  $\pi$ -bonded ethylene adsorbed on gold sites is detected. As the gold coverage decreases to between 0.7 to 0.5,  $\pi$ -bonded ethylene is found on the alloy surface with a heat of adsorption and  $\sigma$ - $\pi$  parameter similar to that found on hydrogen-covered Pd(111). Both the heat of adsorption of ethylene and its  $\sigma$ - $\pi$  parameter increase monotonically as the gold coverage decreases, eventually reaching a value of  $\sim 76 \text{ kJ/mol}$  found for clean palladium, where it adsorbs in a di- $\sigma$  configuration with a  $\sigma$ - $\pi$  parameter of  $\sim 0.8$ .

## Acknowledgement

We gratefully acknowledge support of this work by the US Department of Energy, Division of Chemical Sciences, Office of Basic Energy Sciences, under Grant number DE-FG02-92ER14289.

## References

- [1] Cat. Gold News, Issue 4, Spring, 2003.
- [2] D. Stacchiola, F. Calaza, L. Burkholder, A.W. Schwabacher, M. Neurock, W.T. Tysse, *Angew. Chem. Int. Ed.* 44 (2005) 4572.
- [3] M. Chen, D. Kumar, C.-W. Yi, D.W. Goodman, *Science* 310 (2005) 291.
- [4] C.J. Baddeley, M. Tikhov, C. Hardacre, J.R. Lomas, R.M. Lambert, *J. Phys. Chem.* 100 (1996) 2189.
- [5] D. Mei, E.W. Hansen, M. Neurock, *J. Phys. Chem. B* 107 (2003) 798.
- [6] T. Zheng, D. Stacchiola, H.C. Poon, D.K. Saldin, W.T. Tysse, *Surf. Sci.* 564 (2004) 71.
- [7] R.A. van Santen, M. Neurock, *J. Phys. Chem. B* 104 (2000) 11127.
- [8] Q. Ge, M. Neurock, *Chem. Phys. Lett.* 358 (2002) 377.
- [9] V. Pallasana, M. Neurock, V.S. Lusvardi, J.J. Lerov, D.D. Kragten, R.A. van Santen, *J. Phys. Chem. B* 106 (2002) 1656.
- [10] D. Stacchiola, L. Burkholder, W.T. Tysse, *Surf. Sci.* 511 (2002) 215.
- [11] D. Stacchiola, W.T. Tysse, *Surf. Sci.* 540 (2003) L600.
- [12] M. Kaltchev, A.W. Thompson, W.T. Tysse, *Surf. Sci.* 391 (1997) 145.
- [13] W.J. Wytenburg, R.M. Lambert, *J. Vac. Sci. Tech. A* 10 (1992) 3597.
- [14] P.A. Redhead, *Vacuum* 12 (1962) 203.
- [15] D. Stacchiola, F. Calaza, T. Zheng, W.T. Tysse, *J. Mol. Catal. A* 228 (2005) 35.



- [16] C.-W. Yi, K. Luo, T. Wei, D.W. Goodman, *J. Phys. Chem. B* 109 (2005) 18535.
- [17] B. Pawelec, A.M. Venezia, V. La Parola, E. Cano-Serrano, J.M. Campos-Martin, J.L.G. Fierro, *Appl. Surf. Sci.* 242 (2005) 380.
- [18] C.J. Baddeley, R.M. Ormerod, A.W. Stephenson, R.M. Lambert, *J. Phys. Chem.* 99 (1995) 5146.
- [19] L. Piccolo, A. Piednoir, J.-C. Bertolini, *Surf. Sci.* 592 (2005) 169.
- [20] C.J. Baddeley, C.J. Barnes, A. Wander, R.M. Ormerod, D.A. King, R.M. Lambert, *Surf. Sci.* 314 (1994) 1.
- [21] F. Maroun, F. Ozanam, O.M. Magnussen, R.J. Behm, *Science* 293 (2001) 1811.
- [22] K. Luo, T. Wei, C.-W. Yi, S. Axnanda, D.W. Goodman, *J. Phys. Chem. B* 109 (2005) 23517.
- [23] D.A. Outka, R.J. Madix, *J. Am. Chem. Soc.* 109 (1978) 1708.
- [24] E.M. Stuve, R.J. Madix, *J. Phys. Chem.* 89 (1985) 3183.
- [25] M.F. Mrozek, M.J. Weaver, *J. Phys. Chem. B* 105 (2001) 8931.
- [26] Ü. Ertürk, A. Otto, *Surf. Sci.* 179 (1987) 163.
- [27] W. Akemann, A. Otto, *Langmuir* 11 (1995) 1196.